DFG–Schwerpunktprogramm 1114

Mathematical methods for time series analysis and digital image processing

Diffusion filters and wavelets: What can they learn from each other?

J. Weickert **G. Steidl**

P. Mrázek **M. Welk**

T. Brox

Preprint 77

Preprint Series DFG-SPP 1114

Preprint 77 **January 2005**

The consecutive numbering of the publications is determined by their chronological order.

The aim of this preprint series is to make new research rapidly available for scientific discussion. Therefore, the responsibility for the contents is solely due to the authors. The publications will be distributed by the authors.

Diffusion Filters and Wavelets: What Can They Learn from Each Other?

Joachim Weickert, Gabriele Steidl, Pavel Mrázek, Martin Welk, Thomas Brox

ABSTRACT Nonlinear diffusion filtering and wavelet shrinkage are two methods that serve the same purpose, namely discontinuity-preserving denoising. In this chapter we give a survey on relations between both paradigms when space-discrete or fully discrete versions of nonlinear diffusion filters are considered. For the case of space-discrete diffusion, we show equivalence between soft Haar wavelet shrinkage and total variation (TV) diffusion for 2-pixel signals. For the general case of N-pixel signals, this leads us to a numerical scheme for TV diffusion with many favourable properties. Both considerations are then extended to 2-D images, where an analytical solution for 2×2 pixel images serves as building block for a wavelet-inspired numerical scheme for TV diffusion. When replacing space-discrete diffusion by fully discrete one with an explicit time discretisation, we obtain a general relation between the shrinkage function of a shift-invariant Haar wavelet shrinkage on a single scale and the diffusivity of a nonlinear diffusion filter. This allows to study novel, diffusion-inspired shrinkage functions with competitive performance, to suggest new shrinkage rules for 2-D images with better rotation invariance, and to propose coupled shrinkage rules for colour images where a desynchronisation of the colour channels is avoided. Finally we present a new result which shows that one is not restricted to shrinkage with Haar wavelets: By using wavelets with a higher number of vanishing moments, equivalences to higher-order diffusion-like PDEs are discovered.

1 Introduction

Signal and image denoising is a field where one often is interested in removing noise without sacrificing important structures such as discontinuities. To this end, a large variety of nonlinear strategies has been proposed in the literature including wavelet shrinkage [10] and nonlinear diffusion filtering [18]; see Figure 1. The goal of this chapter is to survey a number of connections between these two techniques and to outline how they can benefit from each other.

While many publications on the connections between wavelet shrinkage

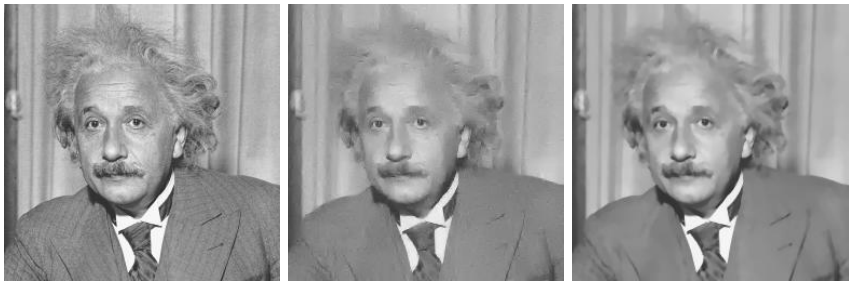

FIGURE 1. **(a) Left:** Original image with additive Gaussian noise. **(b) Middle:** Result after shift invariant soft wavelet shrinkage. **(c) Right:** Result after nonlinear diffusion filtering with total variation diffusivity.

and PDE-based evolutions (as well as related variational methods) focus on the analysis in the *continuous* setting (see e.g. [2, 3, 4, 5, 13]), significantly less investigations have been carried out in the *discrete* setting [7]. In this chapter we give a survey on our contributions that are based on discrete considerations. Due to the lack of space we can only present the main ideas and refer the reader to the original papers [14, 15, 16, 20, 22] for more details.

This chapter is organised as follows: In Section 2 we start with briefly sketching the main ideas behind wavelet shrinkage and nonlinear diffusion filtering. Afterwards in Section 3 we focus on relations between both worlds, when we restrict ourselves to space-discrete nonlinear diffusion with a total variation (TV) diffusivity and to soft Haar wavelet shrinkage. Section 4 presents additional relations that arise from considering fully discrete nonlinear diffusion with arbitrary diffusivities, and Haar wavelet shrinkage with arbitrary shrinkage functions. In Section 5 we present a new result that generalises these considerations to higher-order diffusion-like PDEs and shrinkage with wavelets having a higher number of vanishing moments. The chapter is concluded with a summary in Section 6.

2 Basic Methods

2.1 Wavelet Shrinkage

Wavelet shrinkage has been made popular by a series of papers by Donoho and Johnstone (see e.g. [9, 10]). Assume we are given some discrete 1-D signal $f = (f_i)_{i \in \mathbb{Z}}$ that we may also interpret as a piecewise constant function. Then the *discrete wavelet transform* represents f in terms of shifted versions of a dilated scaling function φ, and shifted and dilated versions of

a wavelet function ψ. In case of orthonormal wavelets, this gives

$$f = \sum_{i\in\mathbb{Z}} \langle f, \varphi_i^n \rangle \, \varphi_i^n + \sum_{j=-\infty}^{n} \sum_{i\in\mathbb{Z}} \langle f, \psi_i^j \rangle \, \psi_i^j, \tag{1.1}$$

where $\psi_i^j(s) := 2^{-j/2}\psi(2^{-j}s - i)$ and where $\langle \cdot, \cdot \rangle$ denotes the inner product in $L_2(\mathbb{R})$. If the measurement f is corrupted by moderate white Gaussian noise, then this noise is contained to a small amount in all wavelet coefficients $\langle f, \psi_i^j \rangle$, while the original signal is in general determined by a few significant wavelet coefficients [12]. Therefore, wavelet shrinkage attempts to eliminate noise from the wavelet coefficients by the following three-step procedure:

1. *Analysis*: Transform the noisy data f to the wavelet coefficients $d_i^j = \langle f, \psi_i^j \rangle$ and scaling function coefficients $c_i^n = \langle f, \varphi_i^n \rangle$ according to (1.1).
2. *Shrinkage*: Apply a shrinkage function S_θ with a threshold parameter θ to the wavelet coefficients, i.e., $S_\theta(d_i^j) = S_\theta(\langle f, \psi_i^j \rangle)$.
3. *Synthesis*: Reconstruct the denoised version u of f from the shrunken wavelet coefficients:

$$u := \sum_{i\in\mathbb{Z}} \langle f, \varphi_i^n \rangle \, \varphi_i^n + \sum_{j=-\infty}^{n} \sum_{i\in\mathbb{Z}} S_\theta(\langle f, \psi_i^j \rangle) \, \psi_i^j. \tag{1.2}$$

In this paper we pay particular attention to *Haar wavelets*, well suited for piecewise constant signals with discontinuities. The Haar wavelet and Haar scaling functions are given respectively by

$$\psi(x) = \mathbf{1}_{[0,\frac{1}{2})} - \mathbf{1}_{[\frac{1}{2},1)}, \tag{1.3}$$

$$\varphi(x) = \mathbf{1}_{[0,1)} \tag{1.4}$$

where $\mathbf{1}_{[a,b)}$ denotes the characteristic function, equal to 1 on $[a, b)$ and zero everywhere else. In the case of the so-called *soft wavelet shrinkage* [9], one uses the shrinkage function

$$S_\theta(s) := \begin{cases} s - \theta \operatorname{sgn} s & \text{if} \quad |s| > \theta, \\ 0 & \text{if} \quad |s| \le \theta. \end{cases} \tag{1.5}$$

2.2 Nonlinear Diffusion Filtering

The basic idea behind nonlinear diffusion filtering [18, 21] in the 1-D case is to obtain a family $u(x, t)$ of filtered versions of a continuous signal $f(x)$ as the solution of a suitable diffusion process

$$u_t = (g(|u_x|) \, u_x)_x \tag{1.6}$$

with f as initial condition,

$$u(x,0) = f(x)$$

and reflecting boundary conditions. Here subscripts denote partial derivatives, and the diffusion time t is a simplification parameter: Larger values correspond to more pronounced filtering.

The diffusivity $g(|u_x|)$ is a nonnegative function that controls the amount of diffusion. Usually, it is decreasing in $|u_x|$. This ensures that strong edges are less blurred by the diffusion filter than low-contrast details. In this chapter, the *total variation (TV)* diffusivity

$$g(|s|) = \frac{1}{|s|} \tag{1.7}$$

plays an important role, since the resulting TV diffusion [1, 8] does not require to specify additional contrast parameters, leads to scale invariant filters, has finite extinction time, interesting shape-preserving qualities, and is equivalent to TV regularisation [19] in the 1-D setting; see the references in [22] for more details.

Unfortunately, TV diffusion is not unproblematic in practice: In corresponding numerical algorithms the unbounded diffusivity requires infinitesimally small time steps or creates very ill-conditioned linear systems. Therefore, TV diffusion is often approximated by a model with bounded diffusivity:

$$u_t \;=\; \left(\frac{1}{\sqrt{\varepsilon^2 + u_x^2}}\, u_x \right)_x \tag{1.8}$$

This regularisation, however, may introduce undesirable blurring effects and destroy some of the favourable properties of unregularised TV diffusion.

3 Relations for Space-Discrete Diffusion

In this section we study connections between soft Haar wavelet shrinkage and nonlinear diffusion with TV diffusivity in the space-discrete case. This allows us to find analytical solutions for simple scenarios. They are used as building blocks for numerical schemes for TV diffusion.

3.1 Equivalence for Two-Pixel Signals

We start by considering wavelet shrinkage of a two-pixel signal (f_0, f_1) in the Haar basis [20]. Its coefficients with respect to the scaling function $\varphi = (\frac{1}{\sqrt{2}}, \frac{1}{\sqrt{2}})$ and the wavelet $\psi = (\frac{1}{\sqrt{2}}, \frac{-1}{\sqrt{2}})$ are given by

$$c \;=\; \frac{f_0 + f_1}{\sqrt{2}}, \qquad d \;=\; \frac{f_0 - f_1}{\sqrt{2}}. \tag{1.9}$$

Soft thresholding of the wavelet coefficient yields

$$S_\theta(d) = \begin{cases} d - \theta \operatorname{sgn} d & \text{if} \quad |d| > \theta, \\ 0 & \text{if} \quad |d| \le \theta, \end{cases} \tag{1.10}$$

leading to the filtered signal (u_0, u_1) with

$$u_0(\theta) = \begin{cases} f_0 + \frac{\theta}{\sqrt{2}} \operatorname{sgn}(f_1 - f_0) & \text{if} \quad \theta < |f_1 - f_0|/\sqrt{2}, \\ (f_0 + f_1)/2 & \text{else}, \end{cases} \tag{1.11}$$

$$u_1(\theta) = \begin{cases} f_1 - \frac{\theta}{\sqrt{2}} \operatorname{sgn}(f_1 - f_0) & \text{if} \quad \theta < |f_1 - f_0|/\sqrt{2}, \\ (f_0 + f_1)/2 & \text{else}. \end{cases} \tag{1.12}$$

On the other hand, space discrete TV diffusion of a two-pixel signal with reflecting boundary conditions and grid size 1 creates the dynamical system

$$\dot{u}_0 = \operatorname{sgn}(u_1 - u_0) \tag{1.13}$$

$$\dot{u}_1 = -\operatorname{sgn}(u_1 - u_0) \tag{1.14}$$

with initial conditions $u_0(0) = f_0$ and $u_1(0) = f_1$. The dot denotes differentiation with respect to time. It is easy to verify that this system with discontinuous right hand side has the unique analytical solution

$$u_0(t) = \begin{cases} f_0 + t \operatorname{sgn}(f_1 - f_0) & \text{if} \quad t < |f_1 - f_0|/2, \\ (f_0 + f_1)/2 & \text{else}, \end{cases} \tag{1.15}$$

$$u_1(t) = \begin{cases} f_1 - t \operatorname{sgn}(f_1 - f_0) & \text{if} \quad t < |f_1 - f_0|/2, \\ (f_0 + f_1)/2 & \text{else}. \end{cases} \tag{1.16}$$

Interestingly, this is equivalent to soft Haar wavelet shrinkage with threshold $\theta = \sqrt{2}t$. Moreover, we observe that a finite extinction time is obvious in the two-pixel model and that no problems with degenerated diffusivities appear [20].

3.2 A Wavelet-Inspired Scheme for TV Diffusion of Signals

Let us now investigate if we can also benefit from the 2-pixel equivalences in the case of general discrete 1-D signals with N pixels. To this end, we perform a wavelet decomposition on the finest scale only. Haar wavelets create natural two-pixel pairings, but unfortunately, their shrinkage is not shift invariant. As a remedy, Coifman and Donoho have proposed to apply *cycle spinning* [6]: On one hand, shrinkage is performed on the original signal. In parallel to this the signal is shifted by 1 pixel, shrinkage is performed, and then the result is shifted back. Averaging both filtered signals creates a process that is shift invariant by construction.

Interestingly this procedure does also inspire a novel numerical scheme for TV diffusion. It uses the analytical solution of the two-pixel model as a

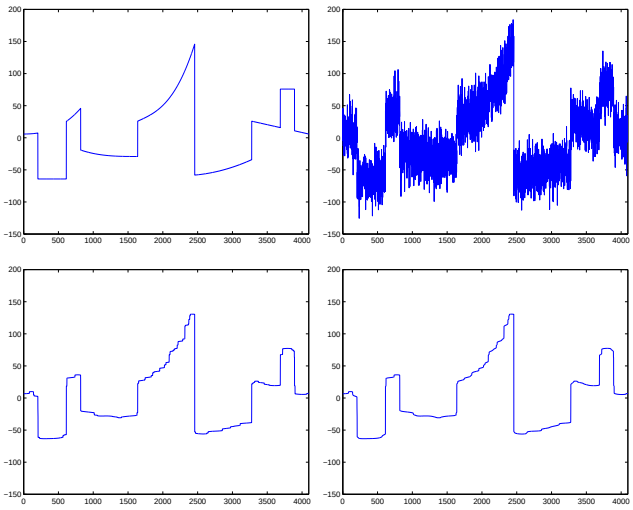

FIGURE 2. **(a) Top left:** Original signal without noise. **(b) Top right:** With additive Gaussian noise, SNR=8 dB. **(c) Bottom left:** Result with two-pixel scheme. SNR = 24.5 dB. **(d) Bottom right:** Result with classical regularised scheme. SNR = 24.6 dB. From [20].

building block. With the two-pixel model, TV diffusion with time step size 2τ is performed on all pixel pairs (u_{2i}, u_{2i+1}). In parallel we perform TV diffusion on all pixel pairs (u_{2i-1}, u_{2i}). Averaging both results leads to the following numerical scheme for TV diffusion [20]:

$$\begin{aligned} u_i^{k+1} \;=\; u_i^k \;&+\; \frac{\tau}{h}\,\mathrm{sgn}\,(u_{i+1}^k - u_i^k)\,\min\left(1,\,\frac{h}{4\tau}|u_{i+1}^k - u_i^k|\right) \\ &-\; \frac{\tau}{h}\,\mathrm{sgn}\,(u_i^k - u_{i-1}^k)\,\min\left(1,\,\frac{h}{4\tau}|u_i^k - u_{i-1}^k|\right), \end{aligned} \tag{1.17}$$

where the upper index k denotes the time level $k\tau$, and h is the spatial grid size. Although this scheme is explicit, it is even absolutely stably since it is based on a linear combination of analytical two-pixel interactions that satisfy a maximum–minimum principle. Moreover, it can be shown that the scheme is also conditionally consistent to the continuous TV diffusion [20]. It should be noted that it does not require any regularisation of the diffusivity such as (1.8), and hence does not suffer from corresponding dissipative artifacts at edges. In Figure 2 it is shown that it is a competitive alternative to conventional schemes based that approximate regularised TV diffusion.

FIGURE 3. (a) Left: Original image, 93×93 pixels. (b) Middle: Standard explicit scheme for regularised TV diffusion ($\varepsilon = 0.01$, $\tau = 0.0025$, 10000 iterations). (c) Right: Same with four-pixel scheme without regularisation ($\tau = 0.1$, 250 iterations). Note that 40 times larger time steps are used. From [22].

3.3 Generalisations to Images

Interestingly, the considerations in Subsections 3.1 and 3.2 can be generalised to the 2-D setting [22]. By considering an image with 2×2 pixels, one shows that soft Haar wavelet shrinkage and space-discrete TV diffusion are equivalent by deriving the same analytical solution for both processes. In order to use this 4-pixel solution as a building block for a numerical scheme for 2-D TV diffusion, we consider the four 2×2 cells containing some pixel (i, j). By computing their analytical solutions and averaging the results, we obtain a wavelet-inspired numerical scheme for 2-D TV diffusion. In the same way as its 1-D counterpart, it is explicit, absolutely stable, conditionally consistent, and does not require any regularisation of the singular TV diffusion equation. Compared to classical explicit discretisations based on regularised TV diffusion, it creates sharper edges, even when significantly larger time step sizes are used; see Figure 3.

4 Relations for Fully Discrete Diffusion

The previous section focused on space-discrete TV diffusion and soft Haar wavelet shrinkage. This restriction allowed us to derive analytical solutions for both paradigms. In order to obtain additonal connections let us now investigate fully discrete nonlinear diffusion with arbitrary diffusivities and Haar wavelet shrinkage with general shrinkage functions.

4.1 Diffusion-Inspired Shrinkage Functions

Let us consider a discrete signal $(f_i)_{i \in \mathbb{Z}}$. It is easily seen that one cycle of shift-invariant Haar wavelet shrinkage on a single level creates a filtered

signal $(u_i)_{i\in\mathbb{Z}}$ with

$$\begin{aligned} u_i &= \frac{f_{i-1}+2f_i+f_{i+1}}{4} + \frac{\sqrt{2}}{4}\,S_\theta\!\left(\frac{f_i-f_{i+1}}{\sqrt{2}}\right) \\ &- \frac{\sqrt{2}}{4}\,S_\theta\!\left(\frac{f_{i-1}-f_i}{\sqrt{2}}\right). \end{aligned} \tag{1.18}$$

On the other hand, the first iteration of an explicit (Euler forward) scheme for a nonlinear diffusion filter with initial state f, time step size τ and spatial step size 1 leads to

$$\frac{u_i-f_i}{\tau} \;=\; g(|f_{i+1}-f_i|)\,(f_{i+1}-f_i) \;-\; g(|f_i^k-f_{i-1}^k|)\,(f_i^k-f_{i-1}^k), \tag{1.19}$$

which can be rewritten as

$$\begin{aligned} u_i &= \frac{f_{i-1}+2f_i+f_{i+1}}{4} + (f_i-f_{i+1})\,\left(\frac{1}{4}-\tau\,g(|f_i-f_{i+1}|)\right) \\ &- (f_{i-1}-f_i)\,\left(\frac{1}{4}-\tau\,g(|f_{i-1}-f_i|)\right). \end{aligned} \tag{1.20}$$

Comparing (1.18) and (1.20) shows that both methods are equivalent if

$$\frac{\sqrt{2}}{4}\,S_\theta\left(\frac{s}{\sqrt{2}}\right) \;=\; s\,\left(\frac{1}{4}-\tau\,g(|s|)\right). \tag{1.21}$$

This formula states a general correspondence between a shrinkage function S_θ of a shift-invariant single scale Haar wavelet shrinkage and the diffusivity g of an explicit nonlinear diffusion scheme [15]. It does not only allow to reinterpret a number of shrinkage strategies as nonlinear diffusion filters (Figure 4), it also leads to novel, diffusion-inspired shrinkage functions (Figure 5). Interestingly, some of these diffusion-inspired shrinkage functions turn out to belong to the ones with the best denoising capabilities [15]. A detailed analysis of this connection in terms of extremum principles, monotonicity preservation and sign stability can be found in [16].

4.2 Wavelet Shrinkage with Improved Rotation Invariance

In order to extend our results from 1-D signals to 2-D greyscale images, we have to specify the 2-D Haar Wavelet transform first. It is based on a lowpass filter L with coefficients $(\frac{1}{\sqrt{2}},\frac{1}{\sqrt{2}})$ and a highpass filter H with coefficients $(\frac{1}{\sqrt{2}},-\frac{1}{\sqrt{2}})$ Applying the 1-D filters L and H alternatingly in x and y direction gives a 2-D Haar wavelet decomposition with the following

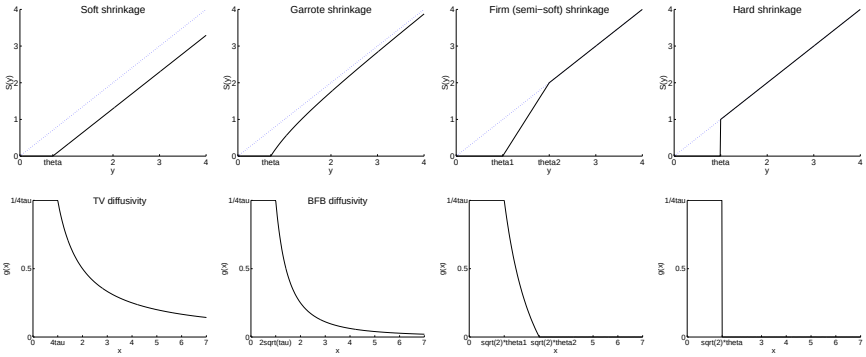

FIGURE 4. **(a) Top:** Four popular shrinkage functions: soft, garrote, firm, and hard shrinkage. **(b) Bottom:** Corresponding diffusivities. From [15].

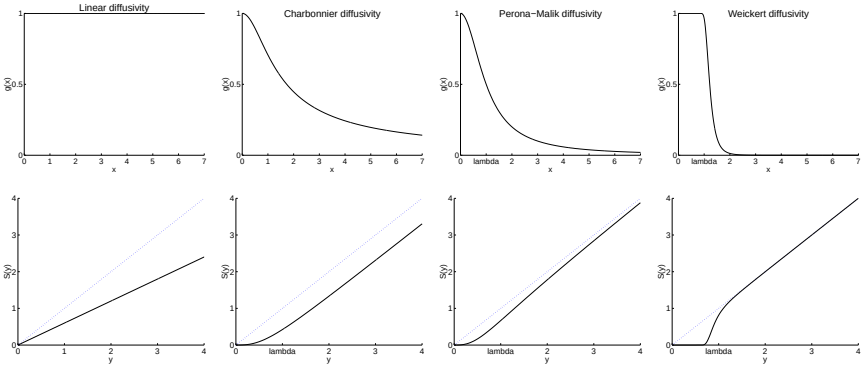

FIGURE 5. **(a) Top:** Four popular diffusivities: linear, Charbonnier, Perona–Malik, and Weickert diffusivity. **(b) Bottom:** Corresponding shrinkage functions. From [15].

FIGURE 6. **(a) Left:** Original image. **(b) Right:** The first three levels of a 2-D Haar wavelet decomposition.

structure:

$$v^{l+1} = L(x) * L(y) * v^l, \tag{1.22}$$

$$w_y^{l+1} = L(x) * H(y) * v^l, \tag{1.23}$$

$$w_x^{l+1} = H(x) * L(y) * v^l, \tag{1.24}$$

$$w_{xy}^{l+1} = H(x) * H(y) * v^l \tag{1.25}$$

with $v^0 := f$. Figure 6 illustrates this principle.

The basic idea behind classical 2-D wavelet shrinkage is now to shrink all wavelet coefficients w_y, w_x and w_{xy} separately according to their magnitude. If shift invariance is required, one averages the results for the 4 shift possibilities. However, even in this case, one usually observes a severe lack of rotation invariance.

In order to address this problem, let us investigate 2-D nonlinear diffusion filtering. In its isotropic variant with a scalar-valued diffusivity [18], it is based on the rotationally invariant equation

$$u_t = \operatorname{div}(g(|\nabla u|)\, \nabla u) \tag{1.26}$$

In a similar way as in the 1-D situation, one can now consider explicit discretisations and relate the diffusivities to shrinkage functions for shift invariant Haar wavelet shrinkage. In contrast to classical shrinkage where the wavelet coefficients are shrunken separately, this leads to novel shrinkage rules where the wavelets are coupled [14], e.g.

$$S(w_x) = w_x \left(1 - 4\,\tau\, g\left(\sqrt{w_x^2 + w_y^2 + 2w_{xy}^2}\right)\right), \tag{1.27}$$

$$S(w_y) = w_y \left(1 - 4\,\tau\, g\left(\sqrt{w_x^2 + w_y^2 + 2w_{xy}^2}\right)\right), \tag{1.28}$$

$$S(w_{xy}) = w_{xy} \left(1 - 4\,\tau\, g\left(\sqrt{w_x^2 + w_y^2 + 2w_{xy}^2}\right)\right). \tag{1.29}$$

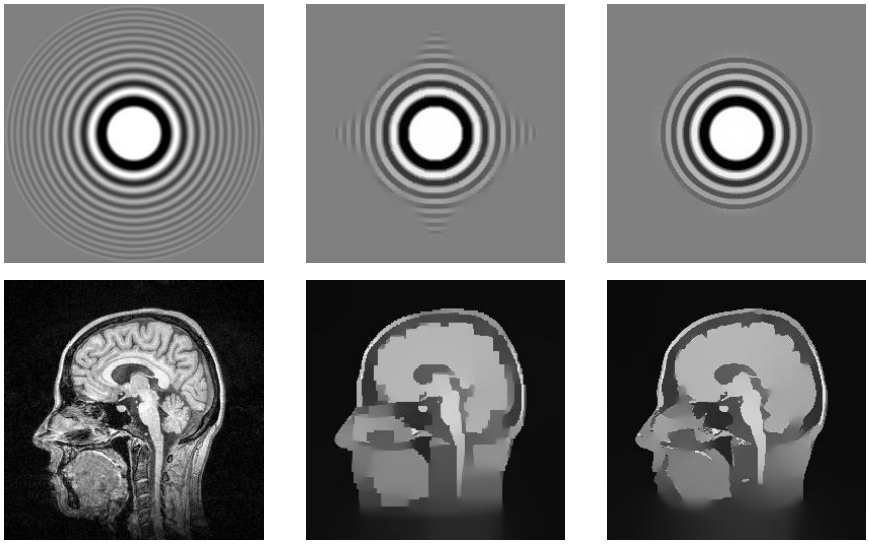

FIGURE 7. (a) **Left:** original images. (b) **Middle:** reconstruction after iterated shift invariant hard wavelet shrinkage. (c) **Right:** reconstruction by a diffusion-inspired wavelet shrinkage with much better rotation invariance. From [14].

Because of the rotation invariance of the nonlinear diffusion equation, one can expect that these shrinkage rules lead to a significantly better realisiation of rotation invariance than classical 2-D wavelet shrinkage. These expectations are confirmed by the experiments in Figure 7.

4.3 Diffusion-Inspired Wavelet Shrinkage of Colour Images

While we have investigated diffusion-inspired shrinkage of greyscale images in the previous section, let us now turn our attention to colour images. In this case wavelet shrinkage is frequently applied such that the different colour channels (e.g. RGB or YUV) are shrunken separately. This can result in a lack of synchronisation that creates artifacts at colour edges.

For nonlinear diffusion filtering of colour images, one often uses a process with a joint diffusivity that steers the evolution of all three channels [11]. In the continuous setting such an evolution has the structure

$$\partial_t u_i = \operatorname{div}\Big(g\Big(\Big(\sum_{j=1}^{3} |\nabla u_j|^2\Big)^{1/2}\Big)\,\nabla u_i\Big) \tag{1.30}$$

where the index i specifies the colour channel. By considering an explicit discretisation and relating it to wavelet shrinkage, we end up with shrinkage rules where all channels are coupled. Figure 8 illustrates that this diffusion-inspired shrinkage of colour images leads to a more convincing behaviour at edges where all channels remain synchronised.

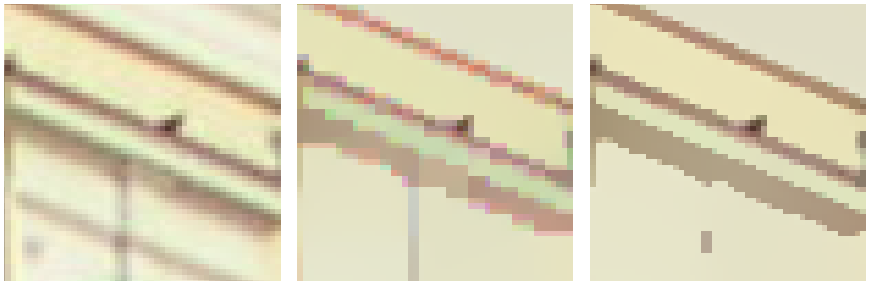

FIGURE 8. **(a) Left:** Zoom into an original image. **(b) Middle:** After classical wavelet shrinkage without coupling the RGB channels. **(c) Right:** Wavelet shrinkage with diffusion-inspired channel coupling.

5 Wavelets with Higher Vanishing Moments

Up to now we have only considered relations between *Haar* wavelet shrinkage and nonlinear diffusion with diffusivities depending on *first* order derivatives. In this section, we will see that there exists also a relation between one step of translation invariant wavelet shrinkage with wavelets having $m \geq 1$ vanishing moments and explicit difference schemes of diffusion-like equations whose diffusivities include m-th order derivatives. To our knowledge these relations have not been considered in the literature before.

For the sake of simplicity, we restrict our attention to the periodic setting, i.e., in the following all indices are taken modulo N. We are concerned with wavelet filters $h^i := (h^i_0, \ldots, h^i_{M_i-1})$, $i = 1, 2$ having the perfect reconstruction property

$$\frac{1}{2}\left(\sum_{k=0}^{M_0-1} h^0_k h^0_{k-l} + \sum_{k=0}^{M_1-1} h^1_k h^1_{k-l}\right) = \delta_{0,l}. \tag{1.31}$$

Moreover, we assume that h^1 has $m \geq 1$ vanishing moments:

$$\sum_{k=0}^{M_1-1} k^r\, h^1_k \;=\; 0, \qquad r = 0, \ldots, m-1, \tag{1.32}$$

$$\sum_{k=0}^{M_1-1} k^m\, h^1_k \;=\; \gamma_m \;\neq\; 0. \tag{1.33}$$

Examples of such filters are for $m = 1$ the Haar filter pair

$$h^0 := \frac{1}{\sqrt{2}}(1, 1), \qquad h^1 := \frac{1}{\sqrt{2}}(1, -1) \tag{1.34}$$

with $\gamma_1 = -1/\sqrt{2}$, and for $m = 2$ the Daubechies filter pair

$$h^0 := \frac{1}{4\sqrt{2}}\left(1+\sqrt{3},\ 3+\sqrt{3},\ 3-\sqrt{3},\ 1-\sqrt{3}\right), \tag{1.35}$$

$$h^1 := \frac{1}{4\sqrt{2}}\left(-1+\sqrt{3},\ 3-\sqrt{3},\ -3-\sqrt{3},\ 1+\sqrt{3}\right) \tag{1.36}$$

with $\gamma_2 = \sqrt{3}/\sqrt{2}$. Then the three steps of wavelet shrinkage applied to the signal $f := (f_0, \ldots, f_{N-1})$ read as follows:

- *Analysis step:* For $j = 0, \ldots, N-1$, we compute

$$c_j := \sum_{k=0}^{M_0-1} h_k^0 f_{k+j} = \sum_{k=0}^{N-1} h_{k-j}^0 f_k, \tag{1.37}$$

$$d_j := \sum_{k=0}^{M_1-1} h_k^1 f_{k+j} = \sum_{k=0}^{N-1} h_{k-j}^1 f_k, . \tag{1.38}$$

- *Shrinkage step:* For $j = 0, \ldots, N-1$ we shrink the highpass coefficients d_j as $S_\theta(d_j)$, $j = 0, \ldots, N-1$.

- *Synthesis step:* For $j = 0, \ldots, N-1$, we compute

$$u_j := \frac{1}{2}\left(\sum_{k=0}^{M_0-1} h_k^0\, c_{j-k} + \sum_{k=0}^{M_1-1} h_k^1\, S_\theta(d_{j-k})\right). \tag{1.39}$$

Assume now that the samples $f_k := f(kh)$ with $h := 1/N$ were taken from a sufficiently smooth periodic function with period 1. Then we obtain by the Taylor expansion that

$$f_{k+l} = \sum_{r=0}^{m} \frac{(kh)^r}{r!} f^{(r)}(lh) + \mathcal{O}(h^{m+1}). \tag{1.40}$$

Since h^1 has m vanishing moments, it follows with (1.38) that

$$\begin{aligned} d_l &= \sum_{r=0}^{m} \frac{h^r}{r!} f^{(r)}(lh) \sum_{k=0}^{M_1-1} k^r\, h_k^1 \ +\ \mathcal{O}(h^{m+1}) \\ &= \frac{h^m}{m!} f^{(m)}(lh)\gamma_m \ +\ \mathcal{O}(h^{m+1}). \end{aligned} \tag{1.41}$$

Thus,

$$f^{(m)}(lh) = \frac{m!}{\gamma_m h^m} d_l \ +\ \mathcal{O}(h). \tag{1.42}$$

Similarly, we conclude that

$$f^{(m)}(lh) = \frac{(-1)^m m!}{\gamma_m h^m} \sum_{k=0}^{M_1-1} h_k^1 f_{l-k} \ +\ \mathcal{O}(h). \tag{1.43}$$

Let us now consider a higher-order diffusion-like equation with periodic boundary conditions:

$$\begin{aligned} u_t &= \left((g(|u^{(m)}|)u^{(m)} \right)^{(m)}, && (1.44)\\ u(x,0) &= f(x), && (1.45)\\ u^{(r)}(0) &= u^{(r)}(1), \qquad r = 0,\dots,2m-1. && (1.46) \end{aligned}$$

We approximate the inner and outer m–th derivatives by (1.42) and (1.43), respectively. This results in

$$u_t(jh) \;\approx\; \frac{(-1)^m (m!)^2}{(\gamma_m h^m)^2} \sum_{k=0}^{M_1-1} h_k^1 \, g\left(\left| \frac{m!}{\gamma_m h^m} \, d_{j-k} \right| \right) d_{j-k}. \tag{1.47}$$

Finally, the approximation of u_t by a forward difference with time step τ leads to an iterative scheme whose first step reads

$$u_j^{(1)} \;:=\; f_j + \tau \frac{(-1)^m (m!)^2}{(\gamma_m h^m)^2} \sum_{k=0}^{M_1-1} h_k^1 \, g\left(\left| \frac{m!}{\gamma_m h^m} \, d_{j-k} \right| \right) d_{j-k}. \tag{1.48}$$

Since our filter pair has the perfect reconstruction property (1.31), we have with $S_\theta(s) = s$ in (1.39) that $u_j = f_j$. Thus, $u_j^{(1)}$ can be rewritten as

$$\begin{aligned} u_j^{(1)} \;=\; & \frac{1}{2} \left(\sum_{k=0}^{M_0-1} h_k^0 \, c_{j-k} + \sum_{k=0}^{M_1-1} h_k^1 d_{j-k} \cdot \right. \\ & \left. \cdot \left(1 + 2\tau \frac{(-1)^m (m!)^2}{(\gamma_m h^m)^2} \, g\left(\left| \frac{m! \, d_{j-k}}{\gamma_m h^m} \right| \right) \right) \right). \end{aligned} \tag{1.49}$$

Comparing this equation with (1.39) we see that the signal obtained by wavelet shrinkage coincides with those of the first step of our iterative scheme if

$$S_\theta\left(\frac{\gamma_m h^m}{m!} s \right) = s \left(\frac{\gamma_m h^m}{m!} + 2\tau \frac{(-1)^m m!}{\gamma_m h^m} \, g\left(|s|\right) \right). \tag{1.50}$$

This fundamental relation generalises (1.21). It gives the connection between the shinkage function S_θ of single scale, shift-invariant wavelet shrinkage with m vanishing moments and the "diffusivity" g of the diffusion-like PDE (1.44) of order $2m$. For $m = 1$ it coincides with our result (1.21) for Haar wavelet shrinkage. For $m = 2$ we obtain

$$S_\theta\left(\frac{\sqrt{3}}{2\sqrt{2}} \, s \right) = s \left(\frac{\sqrt{3}}{2\sqrt{2}} + \tau \frac{4\sqrt{2}}{\sqrt{3}} g(|s|) \right). \tag{1.51}$$

6 Summary

The goal of this chapter was to give a survey on connections between two discontinuity-preserving paradigms for signal and image denoising: wavelet shrinkage and nonlinear diffusion filtering. Unlike most other researchers in this field we focused on discrete connections. It turned out that the wavelet and the diffusion community can indeed learn much from each other.
Focusing on soft Haar wavelet shrinkage and space-discrete TV diffusion, we showed that diffusion filters can benefit from wavelet shrinkage: It was possible to derive wavelet-inspired schemes for TV diffusion that are explicit, absolutely stable, do not require regularisations in order to cope with singularities, and perform favourably.
On the other hand, investigating fully discrete schemes for nonlinear diffusion filtering and its higher-order generalisations allowed us to find a general relation between its diffusivity and the shrinkage function of shift-invariant wavelet shrinkage on a single scale. This led to diffusion-inspired shrinkage functions with competitive performance, to shrinkage rules with improved rotation invariance, and to coupling strategies for wavelet shrinkage of colour images. Hence, also wavelet methods can benefit from diffusion methods.
These connections give rise to the question whether it is also possible to design hybrid methods that benefit from both worlds by attempting to combine the efficiency of wavelet strategies with the quality of diffusion methods. They can be either regarded as iterated shift-invariant wavelet shrinkage methods, or as multiscale diffusion filters. First experiments confirm that this is indeed an interesting class of methods [17]. Performing a theoretical analysis of the connections between single-step multiscale procedures and iterated single scale methods, however, still leads to a lot of challenging questions. They are a topic of our current research.

Acknowledgements

Our research described in this chapter has been partly funded by the projects We 2602/2-1, We 2602/2-2, and We 2602/1-1 of the *Deutsche Forschungsgemeinschaft (DFG)*. This is gratefully acknowledged.

7 References

[1] F. Andreu, V. Caselles, J. I. Diaz, and J. M. Mazón. Qualitative properties of the total variation flow. *Journal of Functional Analysis*, 188(2):516–547, Feb. 2002.

[2] Y. Bao and H. Krim. Towards bridging scale-space and multiscale frame analyses. In A. A. Petrosian and F. G. Meyer, editors, *Wavelets in Signal and Image Analysis*, volume 19 of *Computational Imaging and Vision*, chapter 6. Kluwer, Dordrecht, 2001.

[3] K. Bredies, D. A. Lorenz, P. Maass, and G. Teschke. A partial differential equation for continuous non-linear shrinkage filtering and its application for analyzing MMG data. In F. Truchetet, editor, *Wavelet Applications in Industrial Processing*, volume 5266 of *Proceedings of SPIE*, pages 84–93. SPIE Press, Bellingham, 2004.

[4] A. Chambolle, R. A. DeVore, N. Lee, and B. L. Lucier. Nonlinear wavelet image processing: variational problems, compression, and noise removal through wavelet shrinkage. *IEEE Transactions on Image Processing*, 7(3):319–335, Mar. 1998.

[5] A. Chambolle and B. L. Lucier. Interpreting translationally-invariant wavelet shrinkage as a new image smoothing scale space. *IEEE Transactions on Image Processing*, 10(7):993–1000, 2001.

[6] R. R. Coifman and D. Donoho. Translation invariant denoising. In A. Antoine and G. Oppenheim, editors, *Wavelets in Statistics*, pages 125–150. Springer, New York, 1995.

[7] R. R. Coifman and A. Sowa. New methods of controlled total variation reduction for digital functions. *SIAM Journal on Numerical Analysis*, 39(2):480–498, 2001.

[8] F. Dibos and G. Koepfler. Global total variation minimization. *SIAM Journal on Numerical Analysis*, 37(2):646–664, 2000.

[9] D. L. Donoho. De-noising by soft thresholding. *IEEE Transactions on Information Theory*, 41:613–627, 1995.

[10] D. L. Donoho and I. M. Johnstone. Ideal spatial adaptation by wavelet shrinkage. *Biometrica*, 81(3):425–455, 1994.

[11] G. Gerig, O. Kübler, R. Kikinis, and F. A. Jolesz. Nonlinear anisotropic filtering of MRI data. *IEEE Transactions on Medical Imaging*, 11:221–232, 1992.

[12] S. Mallat. *A Wavelet Tour of Signal Processing*. Academic Press, San Diego, second edition, 1999.

[13] Y. Meyer. *Oscillating Patterns in Image Processing and Nonlinear Evolution Equations*, volume 22 of *University Lecture Series*. AMS, Providence, 2001.

[14] P. Mrázek and J. Weickert. Rotationally invariant wavelet shrinkage. In B. Michaelis and G. Krell, editors, *Pattern Recognition*, volume 2781 of *Lecture Notes in Computer Science*, pages 156–163, Berlin, 2003. Springer.

[15] P. Mrázek, J. Weickert, and G. Steidl. Correspondences between wavelet shrinkage and nonlinear diffusion. In L. D. Griffin and M. Lillholm, editors, *Scale-Space Methods in Computer Vision*, volume 2695 of *Lecture Notes in Computer Science*, pages 101–116, Berlin, 2003. Springer.

[16] P. Mrázek, J. Weickert, and G. Steidl. Diffusion-inspired shrinkage functions and stability results for wavelet denoising. Technical Report 96, Dept. of Mathematics, Saarland University, Saarbrücken, Germany, Oct. 2003. Submitted to *International Journal of Computer Vision*.

[17] P. Mrázek, J. Weickert, G. Steidl, and M. Welk. On iterations and scales of nonlinear filters. In O. Drbohlav, editor, *Proc. Eighth Computer Vision Winter Workshop*, pages 61–66, Valtice, Czech Republic, Feb. 2003. Czech Pattern Recognition Society.

[18] P. Perona and J. Malik. Scale space and edge detection using anisotropic diffusion. *IEEE Transactions on Pattern Analysis and Machine Intelligence*, 12:629–639, 1990.

[19] L. I. Rudin, S. Osher, and E. Fatemi. Nonlinear total variation based noise removal algorithms. *Physica D*, 60:259–268, 1992.

[20] G. Steidl, J. Weickert, T. Brox, P. Mrázek, and M. Welk. On the equivalence of soft wavelet shrinkage, total variation diffusion, total variation regularization, and SIDEs. *SIAM Journal on Numerical Analysis*, 42(2):686–713, 2004.

[21] J. Weickert. *Anisotropic Diffusion in Image Processing*. Teubner, Stuttgart, 1998.

[22] M. Welk, J. Weickert, and G. Steidl. A four-pixel scheme for singular differential equations. In R. Kimmel, N. Sochen, and J. Weickert, editors, *Scale-Space and PDE Methods in Computer Vision*, Lecture Notes in Computer Science, Berlin, 2005. Springer. To appear.

Preprint Series DFG-SPP 1114

http://www.math.uni-bremen.de/zetem/DFG-Schwerpunkt/preprints/

Reports

[1] W. Horbelt, J. Timmer, and H.U. Voss. Parameter estimation in nonlinear delayed feedback systems from noisy data. 2002 May. ISBN 3-88722-530-9.

[2] A. Martin. Propagation of singularities. 2002 July. ISBN 3-88722-533-3.

[3] T.G. Müller and J. Timmer. Fitting parameters in partial differential equations from partially observed noisy data. 2002 August. ISBN 3-88722-536-8.

[4] G. Steidl, S. Dahlke, and G. Teschke. Coorbit spaces and banach frames on homogeneous spaces with applications to the sphere. 2002 August. ISBN 3-88722-537-6.

[5] J. Timmer, T.G. Müller, I. Swameye, O. Sandra, and U. Klingmüller. Modeling the nonlinear dynamics of cellular signal transduction. 2002 September. ISBN 3-88722-539-2.

[6] M. Thiel, M.C. Romano, U. Schwarz, J. Kurths, and J. Timmer. Surrogate based hypothesis test without surrogates. 2002 September. ISBN 3-88722-540-6.

[7] K. Keller and H. Lauffer. Symbolic analysis of high-dimensional time series. 2002 September. ISBN 3-88722-538-4.

[8] F. Friedrich, G. Winkler, O. Wittich, and V. Liebscher. Elementary rigorous introduction to exact sampling. 2002 October. ISBN 3-88722-541-4.

[9] S.Albeverio and D.Belomestny. Reconstructing the intensity of non-stationary poisson. 2002 November. ISBN 3-88722-544-9.

[10] O. Treiber, F. Wanninger, H. Führ, W. Panzer, G. Winkler, and D. Regulla. An adaptive algorithm for the detection of microcalcifications in simulated low-dose mammography. 2002 November. ISBN 3-88722-545-7.

[11] M. Peifer, J. Timmer, and H.U. Voss. Nonparametric identification of nonlinear oscillating systems. 2002 November. ISBN 3-88722-546-5.

[12] S.M. Prigarin and G. Winkler. Numerical solution of boundary value problems for stochastic differential equations on the basis of the gibbs sampler. 2002 November. ISBN 3-88722-549-X.

[13] A. Martin, S.M.Prigarin, and G. Winkler. Exact numerical algorithms for linear stochastic wave equation and stochastic klein-gordon equation. 2002 November. ISBN 3-88722-547-3.

[14] A. Groth. Estimation of periodicity in time series by ordinal analysis with application to speech. 2002 November. ISBN 3-88722-550-3.

[15] H.U. Voss, J. Timmer, and J. Kurths. Nonlinear dynamical system identification from uncertain and indirect measurements. 2002 December. ISBN 3-88722-548-1.

[16] U. Clarenz, M. Droske, and M. Rumpf. Towards fast non-rigid registration. 2002 December. ISBN 3-88722-551-1.

[17] U. Clarenz, S. Henn, M. Rumpf, and K. Witsch. Relations between optimization and gradient flow with applications to image registration. 2002 December. ISBN 3-88722-552-X.

[18] M. Droske and M. Rumpf. A variational approach to non-rigid morphological registration. 2002 December. ISBN 3-88722-553-8.

[19] T. Preußer and M. Rumpf. Extracting motion velocities from 3d image sequences and spatio-temporal smoothing. 2002 December. ISBN 3-88722-555-4.

[20] K. Mikula, T. Preußer, and M. Rumpf. Morphological image sequence processing. 2002 December. ISBN 3-88722-556-2.

[21] V. Reitmann. Observation stability for controlled evolutionary variational inequalities. 2003 January. ISBN 3-88722-557-0.

[22] K. Koch. A new family of interpolating scaling vectors. 2003 January. ISBN 3-88722-558-9.

[23] A. Martin. Small ball asymptotics for the stochastic wave equation. 2003 January. ISBN 3-88722-559-7.

[24] P. Maaß, T. Köhler, R. Costa, U. Parlitz, J. Kalden, U. Wichard, and C. Merkwirth. Mathematical methods for forecasting bank transaction data. 2003 January. ISBN 3-88722-569-4.

[25] D. Belomestny and H. Siegel. Stochastic and self-similar nature of highway traffic data. 2003 February. ISBN 3-88722-568-6.

[26] G. Steidl, J. Weickert, T. Brox, P. Mrázek, and M. Welk. On the equivalence of soft wavelet shrinkage, total variation diffusion, and sides. 2003 February. ISBN 3-88722-561-9.

[27] J. Polzehl and V. Spokoiny. Local likelihood modeling by adaptive weights smoothing. 2003 February. ISBN 3-88722-564-3.

[28] I. Stuke, T. Aach, C. Mota, and E. Barth. Estimation of multiple motions: regularization and performance evaluation. 2003 February. ISBN 3-88722-565-1.

[29] I. Stuke, T. Aach, C. Mota, and E. Barth. Linear and regularized solutions for multiple motions. 2003 February. ISBN 3-88722-566-X.

[30] W. Horbelt and J. Timmer. Asymptotic scaling laws for precision of parameter estimates in dynamical systems. 2003 February. ISBN 3-88722-567-8.

[31] R. Dahlhaus and S. Subba Rao. Statistical inference of time-varying arch processes. 2003 April. ISBN 3-88722-572-4.

[32] G. Winkler, A. Kempe, V. Liebscher, and O. Wittich. Parsimonious segmentation of time series by potts models. 2003 April. ISBN 3-88722-573-2.

[33] R. Ramlau and G. Teschke. Regularization of sobolev embedding operators and applications. 2003 April. ISBN 3-88722-574-0.

[34] K. Bredies, D. Lorenz, and P. Maaß. Mathematical concepts of multiscale smoothing. 2003 April. ISBN 3-88722-575-9.

[35] A. Martin, S.M. Prigarin, and G. Winkler. Exact and fast numerical algorithms for the stochastic wave equation. 2003 May. ISBN 3-88722-576-7.

[36] D. Maraun, W. Horbelt, H. Rust, J. Timmer, H.P. Happersberger, and F. Drepper. Identification of rate constants and non-observable absorption spectra in nonlinear biochemical reaction dynamics. 2003 May. ISBN 3-88722-577-5.

[37] Q. Xie, M. Holschneider, and M. Kulesh. Some remarks on linear diffeomorphisms in wavelet space. 2003 July. ISBN 3-88722-582-1.

[38] M.S. Diallo, M., Holschneider, M. Kulesh, F. Scherbaum, and F. Adler. Characterization of seismic waves polarization attributes using continuous wavelet transforms. 2003 July. ISBN 3-88722-581-3.

[39] T. Maiwald, M. Winterhalder, A. Aschenbrenner-Scheibe, H.U. Voss, A. Schulze-Bonhage, and J. Timmer. Comparison of three nonlinear seizure prediction methods by means of the seizure prediction characteristic. 2003 September. ISBN 3-88722-594-5.

[40] M. Kulesh, M. Holschneider, M.S. Diallo, Q. Xie, and F. Scherbaum. Modeling of wave dispersion using continuous wavelet transforms. 2003 October. ISBN 3-88722-595-3.

[41] A.G.Rossberg, K.Bartholomé, and J.Timmer. Data-driven optimal filtering for phase and frequency of noisy oscillations: Application to vortex flow metering. 2004 January. ISBN 3-88722-600-3.

[42] Karsten Koch. Interpolating scaling vectors. 2004 February. ISBN 3-88722-601-1.

[43] O.Hansen, S.Fischer, and R.Ramlau. Regularization of mellin-type inverse problems with an application to oil engeneering. 2004 February. ISBN 3-88722-602-X.

[44] T.Aach, I.Stuke, C.Mota, and E.Barth. Estimation of multiple local orientations in image signals. 2004 February. ISBN 3-88722-607-0.

[45] C.Mota, T.Aach, I.Stuke, and E.Barth. Estimation of multiple orientations in multidimensional signals. 2004 February. ISBN 3-88722-608-9.

[46] I.Stuke, T.Aach, E.Barth, and C.Mota. Analysing superimposed oriented patterns. 2004 February. ISBN 3-88722-609-7.

[47] Henning Thielemann. Bounds for smoothness of refinable functions. 2004 February. ISBN 3-88722-610-0.

[48] Dirk A. Lorenz. Variational denoising in besov spaces and interpolation of hard and soft wavelet shrinkage. 2004 March. ISBN 3-88722-605-4.

[49] V. Reitmann and H. Kantz. Frequency domain conditions for the existence of almost periodic solutions in evolutionary variational inequalities. 2004 March. ISBN 3-88722-606-2.

[50] Karsten Koch. Interpolating scaling vectors: Application to signal and image denoising. 2004 May. ISBN 3-88722-614-3.

[51] Pavel Mrázek, Joachim Weickert, and Andrés Bruhn. On robust estimation and smoothing with spatial and tonal kernels. 2004 June. ISBN 3-88722-615-1.

[52] Dirk A. Lorenz. Solving variational problems in image processing via projections - a common view on tv denoising and wavelet shrinkage. 2004 June. ISBN 3-88722-616-X.

[53] A.G. Rossberg, K.Bartholomé, H.U. Voss, and J. Timmer. Phase synchronization from noisy univariate signals. 2004 August. ISBN 3-88722-617-8.

[54] Markus Fenn and Gabriele Steidl. Robust local approximation of scattered data. 2004 October. ISBN 3-88722-622-4.

[55] Henning Thielemann. Audio processing using haskell. 2004 October. ISBN 3-88722-623-2.

[56] M.Holschneider, M. S. Diallo, M. Kulesh, F. Scherbaum, M. Ohrnberger, and E. Lück. Characterization of dispersive surface wave using continuous wavelet transforms. 2004 October. ISBN 3-88722-624-0.

[57] M. S. Diallo, M. Kulesh, M. Holschneider, and F. Scherbaum. Instantaneous polarization attributes in the time-frequency domain and wave field separation. 2004 October. ISBN 3-88722-625-9.

[58] Stephan Dahlke, Erich Novak, and Winfried Sickel. Optimal approximation of elliptic problems by linear and nonlinear mappings. 2004 October. ISBN 3-88722-627-5.

[59] Hanno Scharr. Towards a multi-camera generalization of brightness constancy. 2004 November. ISBN 3-88722-628-3.

[60] Hanno Scharr. Optimal filters for extended optical flow. 2004 November. ISBN 3-88722-629-1.

[61] Volker Reitmann and Holger Kantz. Stability investigation of volterra integral equations by realization theory and frequency-domain methods. 2004 November. ISBN 3-88722-636-4.

[62] Cicero Mota, Michael Door, Ingo Stuke, and Erhardt Barth. Categorization of transparent-motion patterns using the projective plane. 2004 November. ISBN 3-88722-637-2.

[63] Ingo Stuke, Til Aach, Erhardt Barth, and Cicero Mota. Multiple-motion estimation by block-matching using markov random fields. 2004 November. ISBN 3-88722-635-6.

[64] Cicero Mota, Ingo Stuke, Til Aach, and Erhardt Barth. Spatial and spectral analysis of occluded motions. 2004 November. ISBN 3-88722-638-0.

[65] Cicero Mota, Ingo Stuke, Til Aach, and Erhardt Barth. Estimation of multiple orientations at corners and junctions. 2004 November. ISBN 3-88722-639-9.

[66] A. Benabdallah, A. Löser, and G. Radons. From hidden diffusion processes to hidden markov models. 2004 December. ISBN 3-88722-641-0.

[67] Andreas Groth. Visualization and detection of coupling in time series by order recurrence plots. 2004 December. ISBN 3-88722-642-9.

[68] M. Winterhalder, B. Schelter, J. Kurths, and J. Timmer. Sensitivity and specificity of coherence and phase synchronization analysis. 2005 January. ISBN 3-88722-648-8.

[69] M. Winterhalder, B. Schelter, W. Hesse, K. Schwab, L. Leistritz, D. Klan, R. Bauer, J. Timmer, and H. Witte. Comparison of time series analysis techniques to detect direct and time-varying interrelations in multivariate, neural systems. 2005 January. ISBN 3-88722-643-7.

[70] B. Schelter, M. Winterhalder, K. Schwab, L. Leistritz, W. Hesse, R. Bauer, H. Witte, and J. Timmer. Quantification of directed signal transfer within neural networks by partial directed coherence: A novel approach to infer causal time-depending influences in noisy, multivariate time series. 2005 January. ISBN 3-88722-644-5.

[71] B. Schelter, M. Winterhalder, B. Hellwig, B. Guschlbauer, C.H. Lücking, and J. Timmer. Direct or indirect? graphical models for neural oscillators. 2005 January. ISBN 3-88722-645-3.

[72] B. Schelter, M. Winterhalder, T. Maiwald, A. Brandt, A. Schad, A. Schulze-Bonhage, and J. Timmer. Testing statistical significance of multivariate epileptic seizure prediction methods. 2005 January. ISBN 3-88722-646-1.

[73] B. Schelter, M. Winterhalder, M. Eichler, M. Peifer, B. Hellwig, B. Guschlbauer, C.H. Lücking, R. Dahlhaus, and J. Timmer. Testing for directed influences in neuroscience using partial directed coherence. 2005 January. ISBN 3-88722-647-X.

[74] Dirk Lorenz and Torsten Köhler. A comparison of denoising methods for one dimensional time series. 2005 January. ISBN 3-88722-649-6.

[75] Esther Klann, Peter Maass, and Ronny Ramlau. Tikhonov regularization with wavelet shrinkage for linear inverse problems. 2005 January.

[76] Eduardo Valenzuela-Domínguez and Jürgen Franke. A bernstein inequality for strongly mixing spatial random processes. 2005 January. ISBN 3-88722-650-X.

[77] J. Weickert, G. Steidl, P. Mrázek, M. Welk, and T. Brox. Diffusion filters and wavelets: What can they learn from each other? 2005 January.